Lattice Relaxation in Oxide Heterostructures: $LaTiO_3/SrTiO_3$ Superlattices

Satoshi Okamoto,[1,*] Andrew J. Millis,[1] and Nicola A. Spaldin[2]

[1]*Department of Physics, Columbia University, 538 West 120th Street, New York, New York 10027, USA*

[2]*Materials Research Laboratory and Materials Department, University of California, Santa Barbara, California, 93106, USA*

(Received 4 January 2006; published 31 July 2006)

Local density approximation + Hubbard U and many-body effective Hamiltonian calculations are used to determine the effects of lattice relaxation in $LaTiO_3/SrTiO_3$ superlattices. Large ferroelectric-like distortions of the TiO_6 octahedra are found, which substantially affect the Ti d-electron density, bringing the calculated results into good agreement with experimental data. The relaxations also change the many-body physics, leading to a novel symmetry-breaking-induced ordering of the xy orbitals, which does not occur in bulk $LaTiO_3$, or in the hypothetical unrelaxed structure.

DOI: 10.1103/PhysRevLett.97.056802 PACS numbers: 73.20.−r, 73.21.Cd, 75.70.−i

Recent advances in the techniques of pulsed laser deposition and molecular beam epitaxy have allowed the creation of ''oxide heterostructures'' consisting of alternating layers, of thickness one or two unit cells, of different transition metal oxide compounds [1,2]. Heterostructures in which one or more of the constituent layers is a material exhibiting correlated electron properties [3,4], such as Mott insulating behavior, high temperature superconductivity or colossal magnetoresistance, are of particular interest, and progress has been made in characterization [5–9] and theoretical analysis [10–15] of such structures. However, the existing literature does not address the crucial issue of lattice relaxation. This is expected to be important because a key feature of heterostructures is ''charge redistribution'' [10]: the flow of electrons from one layer to another driven by the difference in electrochemical potentials between the component materials. The electric fields associated with the resulting dipole layer may be expected to drive significant changes in atomic positions compared with the bulk materials. Further, many experimentally relevant heterostructures involve ferroelectric or nearly ferroelectric materials, for example $SrTiO_3$ with enhanced dielectric response. In this Letter we present the first calculations of lattice relaxation in $LaTiO_3/SrTiO_3$ heterostructures. We show that the lattice distortions are substantial (∼0.15 Å), and have important consequences for the many-body physics, leading, in particular, to new orbitally ordered phases not found in bulk materials.

We used density functional theory to study [001] (m-n) superlattices in which a unit consisting of m planes of $LaTiO_3$ followed by n planes of $SrTiO_3$ layers is repeated in the [001] (z) direction as in the experiments of Ohtomo *et al.* [2]. The lattice constants in the x and y directions were fixed to the experimental value for cubic $SrTiO_3$ (3.91 Å), the substrate used in the experiments [2]. The c axis lattice constant and atomic z coordinates were optimized retaining the tetragonal symmetry of the crystal. We used the projector augmented wave (PAW) approach [16] as implemented in the Vienna *Ab initio* Simulation Package (VASP) [17,18] with a $4 \times 4 \times 4$ k-point grid and an energy cutoff 500 eV, and the rotationally invariant LDA + U method of Liechtenstein *et al.* [19] with $U = 5$ and $J = 0.64$ eV for the Ti d states [20]. For Sr and Ti we used PAW potentials in which semicore s states are treated as valence states (Sr_{sv} and Ti_{sv} in the VASP distribution). For La and O we used standard potentials (La and O in the VASP distribution). In addition, we found that within the LDA the La f states lie only ∼2 eV above the Fermi level, leading to a spurious mixing with the Ti d bands. Since, in practice, the La f bands lie much higher in energy [21] we impose a large $U_f = 11$ eV and $J_f = 0.68$ eV on the La f states. Omitting U_f changes the results, for example, reducing the magnitude of the lattice relaxation by ∼50%.

Figure 1 shows our calculated relaxed-lattice structures for two representative cases: (1–8) and (2–7) heterostructures. The largest structural relaxations occur in the TiO_2 layer at the $LaTiO_3$-$SrTiO_3$ interface ($Ti_{0.5}$ in the upper panel and Ti_1 in the lower panel) and involve a ferroelectric-like distortion in which the negatively charged O and positively charged Ti ions are displaced relative to each other by 0.15 Å in the (1–8) case and 0.18 Å in the (2–7) structure. This distortion produces a local ionic dipole moment which screens the Coulomb field created by the substitution of Sr^{2+} by La^{3+} ions, and also leads to an increase in the z direction Ti-Ti distance by about 0.08 Å. Moving further away from the interface, the magnitude of the ferroelectric-like distortion decays rapidly, while the Ti-Ti distance reverts to a constant value very close to bulk. The sizes of the lattice distortions are comparable for the one- and two-La-layer cases.

An important quantity for physical insight and further theoretical analysis is the conduction-band charge density: loosely speaking, the Ti d occupancy, which is not unambiguously defined with density functional calculations. To obtain this we make use of the fact that within LDA + U the ground state is a highly polarized ferromagnet in which the magnetization density can be ascribed to the conduction bands. Following the procedure used for the total charge density by Ref. [22] we compute the smoothed magnetization density $\bar{m}(z)$ by averaging in the xy plane and smoothing in z over the range $\pm a/2$. We identify the

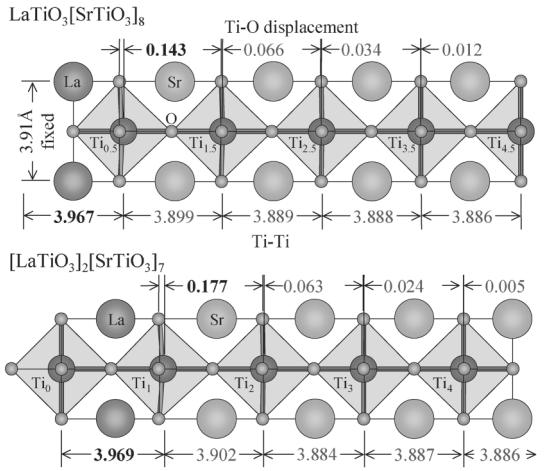

FIG. 1. Calculated optimized lattice structures of superlattices $[LaTiO_3]_1[SrTiO_3]_8$ (upper figure, z-axis lattice constant $c = 35.09$ Å) and $[LaTiO_3]_2[SrTiO_3]_7$ (lower figure, z-axis lattice constant 35.17 Å); half of the unit cell is shown in each case. The intertitanium distances (lower lines) and displacements of the Ti ions relative to the O_2 planes (upper lines) are also indicated. The center of the $LaTiO_3$ region is taken as the zero of the z coordinate in each case and the Ti ions are labeled by their relative z positions.

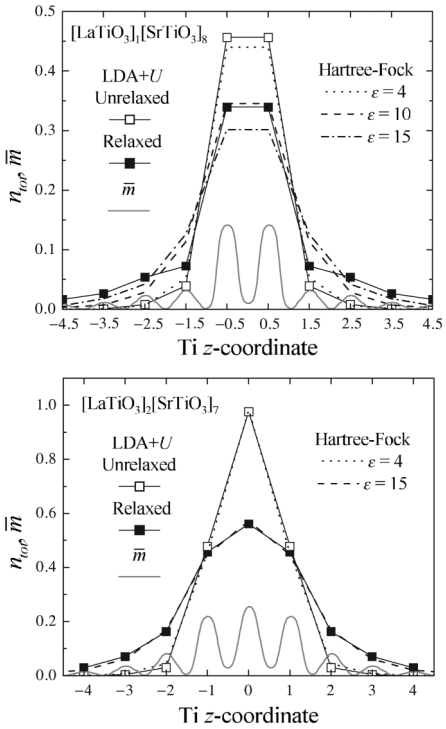

FIG. 2. Charge and magnetization densities for (1–8) and (2–7) heterostructures. Open and filled squares: conduction-band charge densities per unit cell obtained as described in text for unrelaxed and relaxed superlattices, respectively. Light lines: smoothed magnetization densities $\bar{m}(z)$ of relaxed heterostructures. Dotted, dashed, and dash-dotted lines: results of model Hartree-Fock calculation with hopping parameters taken from fits to LDA + U calculations, $U = 5$ and $J = 0.64$ eV, and dielectric constant ε indicated.

integral of $\bar{m}(z)$ over a unit cell with the conduction-band charge density within that unit cell. The total (summed over all cells) conduction-band charge density obtained in this way is within ~1% of the expected 1 electron per La ion in the two-layer structure. The one-layer structure is not quite fully spin polarized: the integral of $\bar{m}$ is ~0.85 electrons; therefore in this case we renormalize the density appropriately.

Figure 2 compares our calculated Ti d charge densities for relaxed (black squares) and unrelaxed (white squares) lattices for $[LaTiO_3]_1[SrTiO_3]_8$ (upper panel) and $[LaTiO_3]_2[SrTiO_3]_7$ (lower panel). In both superlattices, the screening provided by lattice relaxation reduces the charge density on the central Ti layer and produces a long ''tail'' in the charge distribution, extending far away from the interface. The effect is particularly large in the two-layer structure, reducing the middle-layer density by almost a factor of 2. We note that in each case the interface layer ($Ti_{0.5}$ or Ti_1) remains electronically well defined, with the density dropping by approximately 0.3 electrons between the Ti at the interface, and its neighbor surrounded by two Sr-O layers. The relaxed-lattice charge densities agree within experimental uncertainties with the Ti^{3+} values reported by Ohtomo *et al.* [2] both in terms of peak values (0.3–0.4 in the central region) and the slow decay away from the central region.

The lattice relaxations have important consequences for the electronic physics, leading, in particular, to a novel planar xy orbital ordering. To demonstrate this, we show in Fig. 3 the magnetization density (equivalent, as noted above, to the conduction-band charge density) for the unit cell nearest the La layer, averaged over the z direction and presented as contours of constant density. The *butterfly* shape corresponding to xy orbital ordering is evident.

To investigate more precisely the effects of lattice relaxation on the electronic physics we studied a model Hamiltonian with local interactions taken to have the usual Kanamori form [3,10] with $J = 0.64$ eV and the U treated as an adjustable parameter. We also include the Coulomb potentials arising from the La-Sr charge difference and (via the self-consistent Hartree approximation) from the conduction-band charge. We obtain hopping parameters from fits to band calculations.

The heterostructures shown in Fig. 1 have too many bands to make a direct analysis practicable. We observe that the hopping parameters depend on the local environment and that in the structures we consider there are three kinds of Ti sites: those between two La-O planes [e.g. Ti_0 in the (2–7) structure], those between one La-O and Sr-O plane [e.g. $Ti_{0.5}$ in the (1–8) structure], and those between two Sr-O planes. There are correspondingly several different Ti-Ti bonds and thus hopping amplitudes, which we obtain by fitting to bands obtained from LDA + U calcu-

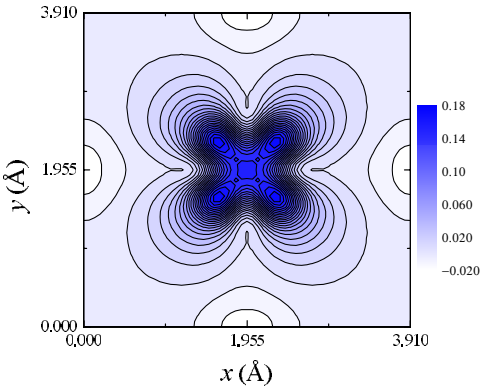

FIG. 3 (color online). Contours of magnetization density in unit cell nearest-to-La plane, integrated over ±1 Å along z direction for relaxed (1–8) heterostructure.

lations for simplified two-layer heterostructures with appropriate choice of counterions and with atomic positions fixed to those found in the full (1–8) or (2–7) relaxed and unrelaxed structures. In these additional band structure calculations we eliminated the on-site Coulomb interaction for the Ti d states to avoid the level splittings induced by orbital ordering, but retained the U_f on La for the reasons described above. The resulting electronic structure is well described by a tight-binding Hamiltonian, H_{el}, involving three orbitals labeled by $\alpha = xy, xz, yz$, representing three t_{2g}-symmetry Ti-O antibonding bands, with on-site energies ε_α and nearest-neighbor hoppings t_α^δ along $\delta = x, y, z$ directions given by the usual Slater-Koster rules (further neighbor hoppings were found to be factors of 5–10 smaller). The hopping parameters are dependent on the layer index l. We have $H_{el} = \sum_l [H_\parallel(z_l) + H_\perp(z_l)]$ with

$$H_\parallel(z_l) = \sum_{\alpha,\vec{k}_\parallel} [-2t_\alpha^x(z_l)\cos k_x - 2t_\alpha^y(z_l)\cos k_y + \varepsilon_\alpha(z_l)] d^\dagger_{\alpha\vec{k}_\parallel}(z_l) d_{\alpha\vec{k}_\parallel}(z_l), \quad (1)$$

$$H_\perp(z_l) = \sum_{\alpha,\vec{k}_\parallel} [-t_\alpha^z(z_l) d^\dagger_{\alpha\vec{k}_\parallel}(z_l) d_{\alpha\vec{k}_\parallel}(z_{l+1}) + \text{H.c.}]. \quad (2)$$

The computed hopping and level splitting parameters for the near-La layers which control the physics are shown in Table I for both relaxed and unrelaxed structures. We see that in general the changes due to relaxation are small; in particular, the level splitting (which acts to favor occupancy of the xz/yz orbitals), although nonzero, is not large enough to have an important effect. The crucial feature of our results is a strong (~20%) suppression of the in-plane hopping amplitude of the xz/yz orbitals, due physically to the noncentrosymmetric oxygen relaxation caused by the ferroelectric-like distortion. It is this feature which drives the xy orbital ordering.

We simulated the screening of the lattice relaxation and the filled electronic bands by a fixed dielectric constant ε, which we adjusted to fit the charge density in the near-La region as shown in Fig. 2. We see that the charge density for the unrelaxed lattices is very well described by $\varepsilon = 4$, while the additional screening from lattice relaxations can be simulated reasonably well by increasing ε to 15. The main deficiency is that the model does not capture the highly enhanced long wavelength dielectric response of $SrTiO_3$ and hence overestimates the rate at which the charge density decays far from the $LaTiO_3$ layer ($n_{\text{tot}} \lesssim 0.05$ region) for the (1–8) heterostructure; this is not important for the results presented below.

TABLE I. Tight-binding parameters for symmetry-inequivalent hoppings in units of eV derived from fits to two-layer heterostructures with atomic positions fixed by LDA + U calculations. Values are given for relaxed (labeled R) and unrelaxed (labeled U) $[LaTiO_3]_1[SrTiO_3]_8$ (labeled 1) and $[LaTiO_3]_2[SrTiO_3]_7$ (labeled 2) heterostructures and presented for Ti layers 0.5 or 0, 1 (see Fig. 1) nearest to La-O planes. For larger z_l the hoppings and level splittings are essentially identical to the bulk $SrTiO_3$ values $t_{xy}^{x,y} = t_{xz}^{x,z} = t_{yz}^{y,z} = 0.5$ eV and $\varepsilon_\alpha = 0$.

	$t_{xy}^{x,y}$		t_{xz}^{x}		t_{xz}^{z}		ε_{xy}		ε_{xz}	
z_l	⋯	0.5	⋯	0.5	−0.5	0.5	⋯	0.5	⋯	0.5
1 R	⋯	0.53	⋯	0.46	0.44	0.57	⋯	0.23	⋯	0.19
1 U	⋯	0.55	⋯	0.55	0.56	0.51	⋯	0.27	⋯	0.36
z_l	0	1	0	1	0	1	0	1	0	1
2 R	0.63	0.53	0.63	0.38	0.47	0.58	0.66	0.06	0.66	−0.07
2 U	0.63	0.55	0.63	0.55	0.59	0.51	0.66	0.27	0.66	0.36

Figure 4 displays the ground state phase diagrams for relaxed and unrelaxed heterostructures, computed using hopping parameters and dielectric constants given above and the Hartree-Fock approximation. This approximation, although poor for the excitation spectrum and for $T > 0$, gives a reliable representation of the ground state phase diagram, including the natures of the various ordered phases and their approximate locations in parameter space. For example, for strong coupling insulating phases it gives results in quantitative agreement with superexchange calculations, and for partially filled orbitally degenerate cases it yields the expected ferromagnetism. To avoid complexity coming from the interference between different La regions we studied isolated heterostructures in which n $LaTiO_3$ layers are sandwiched by a semi-infinite number of $SrTiO_3$ layers. The lattice relaxation affects the phase diagram mainly via the changed density profile, shifting the phase boundaries to higher U values and disfavoring the OO-G phase, which is replaced by the ferro-orbital Oxy phase discussed above. We note that the Oxy phase is not found in the unrelaxed structure even at $n = 1$ because the central $Ti_{\pm 0.5}$ charge density is too high. Instead the system prefers other orbitally ordered states with narrower xy plane band widths.

To summarize, we have combined density functional and Hartree-Fock methods to demonstrate the crucial effects of lattice relaxation on $LaTiO_3/SrTiO_3$ superlattices. The essential effect is a large polar distortion of the TiO_6

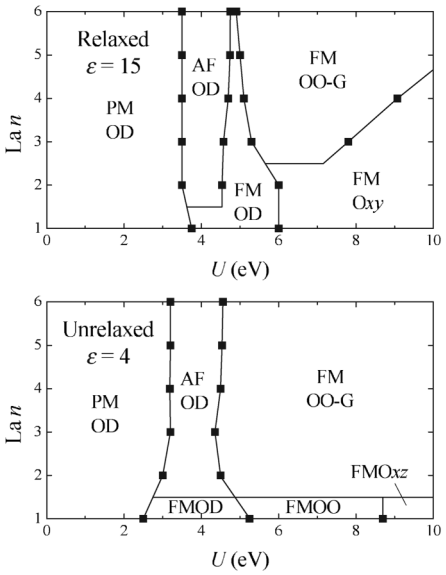

FIG. 4. Spin and orbital phase diagrams of realistic three-band model heterostructures as a function of the intraorbital Coulomb interaction U and La layer thickness n, computed within the Hartree-Fock approximation with interorbital Coulomb interaction $U' = U - 2J$ and exchange interaction $J = 0.64$ eV. Upper panel: relaxed structure with $\varepsilon = 15$ and appropriate band parameters obtained from LDA + U, lower panel: unrelaxed structure with $\varepsilon = 4$. PM: paramagnetic state, FM: ferromagnetic state, AF: antiferromagnetic state in which the magnetic moment alternates from plane to plane, OD: orbitally disordered state, OO-G: orbitally ordered state in which xz and yz orbitals alternate in x, y, and z directions, Oxy(xz): orbitally ordered state in which xy (xz or yz) occupancy is predominant, and OO: orbitally ordered state in which xz and yz orbitals alternate in the z direction.

octahedra in the near-La region, leading to screening which substantially spreads out the conduction-band charge profile, reducing the central layer charge density and creating a long tail away from the La layers. The conduction-band charge densities we find agree very well with experiment, and the distortions also imply a novel ferro-orbital xy ordering.

We thank A. M. Rappe, C. Ederer, and D. R. Hamann for helpful discussions. S. O. acknowledges the Materials Research Laboratory, UC Santa Barbara for kind hospitality. We acknowledge support from the DOE Grant No. ER 46169 (A. M. and S. O.), by the NSF under Grant No. CHE-0434567 (N. S.), and MRL Central Facilities supported by the MRSEC Program of the National Science Foundation under Grant No. DMR05-20415.

Note added.—After this paper was submitted a paper appeared [23] reporting results obtained within the GGA approximation to density functional theory (without U). Lattice distortions similar to those reported here were found; but a small *overscreening* of the La charge occurred, leading to a charge density peak in the middle of the heterostructure.

*Electronic address: okapon@phys.columbia.edu

[1] M. Izumi, Y. Ogimoto, Y. Konishi, T. Manako, M. Kawasaki, and Y. Tokura, Mater. Sci. Eng. B **84**, 53 (2001), and references therein.
[2] A. Ohtomo, D. A. Muller, J. L. Grazul, and H. Y. Hwang, Nature (London) **419**, 378 (2002).
[3] M. Imada, A. Fujimori, and Y. Tokura, Rev. Mod. Phys. **70**, 1039 (1998).
[4] Y. Tokura and N. Nagaosa, Science **288**, 462 (2000).
[5] H. Yamada, Y. Ogawa, Y. Ishii, H. Sato, M. Kawasaki, H. Akoh, and Y. Tokura, Science **305**, 646 (2004).
[6] C. W. Schneider, S. Hembacher, G. Hammerl, R. Held, A. Schmehl, A. Weber, T. Kopp, and J. Mannhart, Phys. Rev. Lett. **92**, 257003 (2004).
[7] J. Stahn, J. Chakhalian, Ch. Niedermayer, J. Hoppler, T. Gutberlet, J. Voigt, F. Treubel, H-U. Habermeier, G. Cristiani, B. Keimer, and C. Bernhard, Phys. Rev. B **71**, 140509(R) (2005).
[8] G. Yu. Logvenov, C. W. Schneider, J. Mannhart, and S. Yu. Barash, Appl. Phys. Lett. **86**, 202505 (2005).
[9] J. J. Kavich, M. P. Warusawithana, J. W. Freeland, P. Ryan, X. Zhai, R. H. Kodama, and J. N. Eckstein, cond-mat/0512158.
[10] S. Okamoto and A. J. Millis, Nature (London) **428**, 630 (2004); Phys. Rev. B **70**, 075101 (2004).
[11] S. Okamoto and A. J. Millis, Phys. Rev. B **70**, 241104(R) (2004).
[12] S. Okamoto and A. J. Millis, Phys. Rev. B **72**, 235108 (2005).
[13] Z. S. Popovic and S. Satpathy, Phys. Rev. Lett. **94**, 176805 (2005).
[14] J. K. Freericks, Phys. Rev. B **70**, 195342 (2004).
[15] N. Pavlenko and T. Kopp, Phys. Rev. B **72**, 174516 (2005).
[16] P. E. Blochl, Phys. Rev. B **50**, 17 953 (1994).
[17] G. Kresse and J. Furthmuller, Phys. Rev. B **54**, 11 169 (1996).
[18] G. Kresse and D. Joubert, Phys. Rev. B **59**, 1758 (1999).
[19] A. I. Liechtenstein, V. I. Anisimov, and J. Zaanen, Phys. Rev. B **52**, R5467 (1995).
[20] T. Mizokawa and A. Fujimori, Phys. Rev. B **51**, R12880 (1995).
[21] M. T. Czyżyk and G. A. Sawatzky, Phys. Rev. B **49**, 14 211 (1994).
[22] N. Sai, A. M. Kolpak, and A. M. Rappe, Phys. Rev. B **72**, 020101(R) (2005).
[23] D. R. Hamann, D. A. Muller, and H. Y. Hwang, Phys. Rev. B **73**, 195403 (2006).